

Manuscript Number: CARBPOL-D-14-01526R2

Title: Polysaccharide-based aerogel microspheres for oral drug delivery

Article Type: Research Paper

Keywords: polysaccharide-based aerogel; ketoprofen; benzoic acid; supercritical impregnation; drug release kinetics

Corresponding Author: Dr. Carlos A García-González,

Corresponding Author's Institution: University of Santiago de Compostela

First Author: Carlos A García-González

Order of Authors: Carlos A García-González; Ming Jin; Joachim Gerth; Carmen Álvarez-Lorenzo; Irina Smirnova

Abstract: Polysaccharide-based aerogels in the form of microspheres were investigated as carriers of poorly water soluble drugs for oral administration. These bio-based carriers may combine the biocompatibility of polysaccharides and the enhanced drug loading capacity of dry aerogels. Aerogel microspheres from starch, pectin and alginate were loaded with ketoprofen (anti-inflammatory drug) and benzoic acid (used in the management of urea cycle disorders) via supercritical CO₂-assisted adsorption. Amount of drug loaded depended on the aerogel matrix structure and composition and reached values up to 1.0×10^{-3} and 1.7×10^{-3} g/m² for ketoprofen and benzoic acid in starch microspheres. After impregnation, drugs were in the amorphous state in the aerogel microspheres. Release behavior was evaluated in different pH media (pH 1.2 and 6.8). Controlled drug release from pectin and alginate aerogel microspheres fitted Gallagher-Corrigan release model ($R^2 > 0.99$ in both cases), with different relative contribution of erosion and diffusion mechanisms depending on the matrix composition. Release from starch aerogel microspheres was driven by dissolution, fitting the first-order kinetics due to the rigid starch aerogel structure, and showed different release rate constant (k_1) depending on the drug (0.075 and 0.160 min⁻¹ for ketoprofen and benzoic acid, respectively). Overall, the results point out the possibilities of tuning drug loading and release by carefully choosing the polysaccharide used to prepare the aerogels.

HIGHLIGHTS

- Polysaccharide aerogel microspheres are investigated as carriers of drugs for oral administration
- Aerogels were loaded with ketoprofen and benzoic acid, poorly water soluble model drugs
- Starch, with the lowest specific surface area, was more prone to adsorb drug molecules
- Release of ketoprofen from alginate and pectin aerogel particles was sensitive to pH of the medium
- Results point out the possibilities of polysaccharide aerogels of tuning drug loading and release

1 **Polysaccharide-based aerogel microspheres for oral drug delivery**

2

3 C.A. García-González^{a,b,*,†}, M. Jin^{b,†}, J. Gerth^c, C. Alvarez-Lorenzo^a, I. Smirnova^{b,**}

4 ^a *Departamento de Farmacia y Tecnología Farmacéutica, Facultad de Farmacia, Universidad de*

5 *Santiago de Compostela, E-15782-Santiago de Compostela, Spain*

6 *Phone: +34 981 63100 (ext. 15252). Fax: +34981 547148*

7 ^b *Institute of Thermal Separation Processes, Hamburg University of Technology*

8 *Eißendorferstraße 38, D-21073 Hamburg, Germany*

9 ^c *Institute of Environmental Technology and Energy Economics, Hamburg University of Technology*

10 *Eißendorferstraße 40, D-21073 Hamburg, Germany*

11

12 *Corresponding authors: * carlos.garcia@usc.es, ** irina.smirnova@tuhh.de*

13 [†] *These authors contributed equally to this work*

14

15

16

17

18 **Abstract**

19 Polysaccharide-based aerogels in the form of microspheres were investigated as carriers of poorly
20 water soluble drugs for oral administration. These bio-based carriers may combine the
21 biocompatibility of polysaccharides and the enhanced drug loading capacity of dry aerogels. Aerogel
22 microspheres from starch, pectin and alginate were loaded with ketoprofen (anti-inflammatory drug)
23 and benzoic acid (used in the management of urea cycle disorders) via supercritical CO₂-assisted
24 adsorption. Amount of drug loaded depended on the aerogel matrix structure and composition and
25 reached values up to 1.0×10^{-3} and 1.7×10^{-3} g/m² for ketoprofen and benzoic acid in starch
26 microspheres. After impregnation, drugs were in the amorphous state in the aerogel microspheres.
27 Release behavior was evaluated in different pH media (pH 1.2 and 6.8). Controlled drug release from
28 pectin and alginate aerogel microspheres fitted Gallagher-Corrigan release model ($R^2 > 0.99$ in both
29 cases), with different relative contribution of erosion and diffusion mechanisms depending on the
30 matrix composition. Release from starch aerogel microspheres was driven by dissolution, fitting the
31 first-order kinetics due to the rigid starch aerogel structure, and showed different release rate constant
32 (k_1) depending on the drug (0.075 and 0.160 min⁻¹ for ketoprofen and benzoic acid, respectively).
33 Overall, the results point out the possibilities of tuning drug loading and release by carefully choosing
34 the polysaccharide used to prepare the aerogels.

35 **Keywords:** polysaccharide-based aerogel; ketoprofen; benzoic acid; supercritical impregnation; drug
36 release kinetics

37

38 **1 Introduction**

39 Bio-based materials may become key formulation ingredients for the engineering of delivery systems
40 able to overcome the biopharmaceutical and stability limitations shown by a number of well-
41 established drugs and new chemical entities (García-González, Alnaief & Smirnova, 2011; García-
42 González, Argemí, Sousa, Duarte, Saurina & Domingo, 2010; Pose-Vilarnovo et al., 2004). Natural
43 polysaccharides and/or their derivatives are especially attractive because of their availability,
44 renewability, low toxicity, stability upon storage, good biological performance, and enzyme-controlled
45 biodegradability (Baldwin & Kiick, 2010; Dumitriu, 2012; García-González, Alnaief & Smirnova,
46 2011; Veronovski, Knez & Novak, 2013). Technological advances in extraction and purification
47 processes enable the cost-effective obtaining of natural polysaccharides in large-scale, rendering them
48 interesting for life science applications, e.g., pharmacy, tissue engineering and environmental
49 remediation (Alvarez-Lorenzo, Blanco-Fernandez, Puga & Concheiro, 2013; Baldwin & Kiick, 2010;
50 Kayser, Müller, García-González, Smirnova, Leitner & Domínguez de María, 2012). Several
51 polysaccharide-based drug delivery systems (e.g., Lupron Depot[®] and Nutropin Depot[®]) can already
52 be found in the market (Kim & Pack, 2006).

53 Polysaccharide-based aerogels for drug delivery and biomedical systems were firstly proposed by
54 Berg et al. (Berg, Droege, Fellmann, Klaveness & Rongved, 1995) and since then there has been an
55 increasing interest on the research of these materials for pharmaceutical technology purposes (García-
56 González, Alnaief & Smirnova, 2011; Ulker & Erkey, 2014). Aerogel technology provides high
57 added-value lightweight materials with outstanding surface area and open porosity, suitable to be
58 loaded with active substances. Organic aerogels prepared with US Food and Drug Administration
59 (FDA)- and European Medicines Agency (EMA)-approved bio-based polysaccharides offer unique
60 features as drug carriers by combining the intrinsic properties of the aerogel structure and those of the
61 polysaccharides. Moreover, aerogel carriers may load high amounts of drugs, improve their stability,
62 and control the crystalline form of the drug (García-González & Smirnova, 2013; Smirnova,
63 Suttiruengwong & Arlt, 2004). Drug loading within starch aerogels has been reported to be in the
64 range $1-4 \times 10^{-3} \text{ g/m}^2$ for ibuprofen in starch aerogel monoliths (Mehling, Smirnova, Guenther &
65 Neubert, 2009) or ketoprofen in starch aerogel particles (García-González & Smirnova, 2013), which

66 is larger than the values obtained for silica aerogels ($3.8 \times 10^{-4} \text{ g/m}^2$), an aerogel reference material.
67 Using the supercritical fluid-assisted drug impregnation, drugs are loaded in a non-crystalline form
68 (Mehling, Smirnova, Guenther & Neubert, 2009). Accordingly, ibuprofen and ketoprofen-loaded
69 organic aerogel monoliths and beads (corn starch and alginate) showed faster drug dissolution rate
70 than the crystalline drug (Del Gaudio, Auriemma, Mencherini, Porta, Reverchon & Aquino, 2013;
71 Mehling, Smirnova, Guenther & Neubert, 2009).

72 Aerogels produced in the form of microspheres (Valentin, Molvinger, Quignard & Di Renzo, 2005)
73 are preferred as drug carriers to other aerogel formats, such as monoliths (García-González, Camino-
74 Rey, Alnaief, Zetzl & Smirnova, 2012), granules (Hong, Yoon & Hwang, 2011), powders (Bhagat,
75 Park, Kim, Kim & Han, 2008) or beads (Sarawade, Kim, Hilonga, Quang, Jeon & Kim, 2011). This
76 preference for the microspherical form arises from its high flowability, ease of handling, and improved
77 processing reproducibility coupled to reduced triggering of inflammatory response due to the inherent
78 absence of sharp edges (Hong, Yoon & Hwang, 2011; Radin, Chen & Ducheyne, 2009). Release of
79 active pharmaceutical ingredients (API) from microspheres is a complex process being influenced by
80 various factors that could lead to totally different release profiles. Porous network collapse of aerogel
81 carriers once in contact with aqueous medium notably influences API release. Erosion (by dissolution
82 or hydrolysis) rate depends on the structure and the molecular weight of the polymer, the morphology
83 and size of the carrier, as well as the medium conditions (pH, temperature, enzymes). Polymeric
84 microspheres may erode from the bulk (homogeneous) or from carrier surface (heterogeneous)
85 depending on the relative ratio of water penetration rate to polymer network hydrolysis rate being high
86 or low, respectively, (Rothstein, Federspiel & Little, 2009; von Burkersroda, Schedl & Göpferich,
87 2002) thus influencing the API release into the environment (Kim & Pack, 2006; O'Donnell &
88 McGinity, 1997). Finally, chemical interactions between the drug and the carrier may also influence
89 the release rate.

90 There is still a paucity of information about the effect of the polysaccharide source used to prepare
91 microspherical aerogels on their ability to load and to control the release of active substances.
92 Polysaccharide nature may likely influence the aerogel collapse and, subsequently, the mass transport
93 and release profile of the drug contained in the aerogel as well. The aim of this work was to evaluate

94 the drug loading and release behavior of aerogel microspheres prepared from three polysaccharides
95 (starch, alginate, and pectin) according to an emulsion-gelation method followed by supercritical
96 drying, in order to elucidate their potential as carriers of poorly water soluble drugs for oral
97 administration. Ketoprofen and benzoic acid were loaded into the aerogels by supercritical (sc)CO₂
98 fluid-assisted impregnation. Silica aerogel microspheres were used as aerogel reference regarding drug
99 loading capacity and release for the sake of comparison. Drug release kinetics from polysaccharide
100 aerogel microspheres were evaluated at gastric and intestinal pH conditions. To the best of our
101 knowledge, this work represents the first systematic study in the fast developing field of the
102 microformulation of supports for drug release using aerogels in the form of microspheres as drug
103 carrier.

104 **2 Materials and methods**

105 2.1 Reagents

106 Native corn starch (Starch amylo N-460; 52.6% amylose content) was from Roquette (France); alginic
107 acid sodium salt (brown algae origin, G/M ratio of 70/30, MW 403,000 g·mol⁻¹) from Sigma Aldrich
108 (Germany); citrus high methoxyl pectin (63-66% degree of esterification, MW 30,000-100,000 g·mol⁻¹)
109 and tetramethoxysilane (TMOS, purity of 98%) from Fluka (Germany). Methanol (95%), hydrochloric
110 acid (30%), ammonium hydroxide (25%) and benzoic acid (98%) were from Merck (Germany).
111 Ketoprofen (racemic mixture) was from Chemische Fabrik Kreussler & Co. GmbH (Germany).
112 Ethanol (99.8%) was from Omnilab (Germany) and domestic grade rapeseed oil was purchased from
113 Brökelmann Co. (Germany). Carbon dioxide was supplied by AGA Gas GmbH (Germany).

114 2.2 Preparation of spherical aerogel microspheres

115 Aerogel microspheres were obtained applying an emulsion-gelation method followed by supercritical
116 drying. In brief, this method consisted on the preparation of a water-in-oil emulsion (or ethanol-in-oil
117 for silica gel microspheres) followed by the gelation of the dispersed phase (thermal gelation for starch
118 and chemical gelation for alginate, pectin and silica) as previously reported (Alnaief, Alzaitoun,
119 García-González & Smirnova, 2011; Alnaief & Smirnova, 2011; García-González, Uy, Alnaief &
120 Smirnova, 2012). Gel microspheres were isolated through centrifugation and exposed to ethanol for

121 solvent exchange. Finally, aerogel microspheres were obtained by scCO₂-assisted drying. The
122 operating conditions used in this work for the preparation of aerogel microspheres correspond to the
123 ones reported in the literature leading to the highest (or close to the highest) specific surface area
124 values so far for each aerogel case using processing approaches compatible with the intended
125 application (i.e., oral drug delivery). Operating conditions for the processing of the aerogel
126 microspheres were chosen so that mean pore diameters in the range 14-18 nm were obtained in all
127 cases to neglect the effect of this variable in the study. For more detailed instructions on the
128 preparation of the aerogels, please refer to the Appendix A in Supplementary Data section.

129 2.3 Ketoprofen and benzoic acid supercritical impregnation

130 Alginate, starch, silica or pectin aerogel microspheres (0.12 g) and active compounds (0.12 g of
131 ketoprofen or benzoic acid) were wrapped separately in filter paper cartridges. Then, a set of two
132 cartridges (one containing microspheres and the other with the drug) were placed in one of the reactors
133 of the apparatus sketched in Figure 1. Control trials (one reactor containing a drug cartridge alone and
134 other containing one cartridge for each aerogel type) were carried out in the two remaining reactors.
135 Experiments were carried out in duplicate. The supercritical impregnation setup used for these
136 experiments not only provides a high-throughput trial program by means of its six reactors arranged in
137 parallel (namely, six experiments can be carried out at the same time), but also improves the
138 reproducibility of the experiments since all trials from the same batch series share the same CO₂
139 pressurization/depressurization cycle and heat transfer histories. scCO₂-assisted impregnation
140 conditions were optimized for ketoprofen (40 °C, 18.0 MPa) and benzoic acid (55 °C, 18.0 MPa)
141 following guidelines of solubility of active compounds in scCO₂ (Jin, Zhong, Zhang & Li, 2004; Stassi,
142 Bettini, Gazzaniga, Giordano & Schiraldi, 2000). Impregnation times were chosen long enough (24h)
143 to neglect the effect of aerogel microparticle size in the drug loading achieved. Impregnation
144 conditions were kept constant under agitation at 500 rpm.

145 2.4 Aerogel microsphere characterization

146 Specific surface area of the bare aerogel microspheres was quantified from low-temperature N₂
147 adsorption-desorption data (Nova 3000e, Quantachrome, USA). Prior to measurements, samples were

148 dried for 20 h under vacuum (<1 mPa) at 60°C for alginate and pectin, 80°C for starch and 200°C for
149 silica aerogels. Mean particle size of wet gel microspheres dispersed in ethanol was estimated by
150 means of laser diffraction spectrometry (Beckman Coulter LS1332) and using similar obscuration
151 values (9-11%) for all samples. Morphology of the polysaccharide aerogel microspheres as well as
152 silica microspheres was evaluated using scanning electron microscopy (SEM, Leo Zeiss 1530,
153 Germany). Morphology and physical integrity of aerogels in contact with water were monitored with
154 aid of high-speed camera by depositing 100 picoliter-water droplets on microsphere surfaces (DSA
155 100M provided by Krüss GmbH, Germany). X-ray diffraction analysis (XRD, Siemens D500
156 diffractometer equipped with a diffracted beam monochromator, Germany) of the drug-loaded and
157 unloaded microspheres as well as aerogel-plus-drug physical mixtures was carried out using a
158 position-sensitive detector and CuK α radiation within the range of 2° to 40° 2 θ and a step size of 0.05°.
159 For determination of drug entrapment efficiency, drug-loaded microspheres (10-50 mg) were
160 dispersed in a known volume of ethanol (sink conditions) and sonicated for 30 min, which was
161 enough for complete drug release. Afterwards the solution was filtered through a 0.22 μ m membrane
162 filter (Millipore syringe filter, PTFE, EW-29950-42, Cole-Parmer, USA) and the absorbance at 255
163 nm (ketoprofen) or 227 nm (benzoic acid) measured (Evolution 300 UV spectrophotometer, Thermo
164 Scientific, USA).

165 2.5 *In vitro* drug release

166 Dissolution test was conducted according to the Ph. Eur. guidelines in 0.1 M phosphate buffer saline
167 (PBS, simulated intestinal fluid, pH 6.8) or in 0.1 N HCl (simulated gastric fluid, pH 1.2) solutions
168 using a paddle apparatus (Sotax At7, Allschwil, Switzerland) with a constant agitation speed of 100
169 rpm at 37 °C. Drug-loaded aerogel microspheres (20-50 mg) were immersed in jars containing 900 mL
170 buffer medium (sink conditions). Samples (2 mL) were withdrawn at determined time intervals and
171 filtered through a 0.22 μ m membrane filter. Each drug release test lasted for 24 h and was run in
172 duplicate. Drug concentration was determined by means of UV spectrophotometry, as described in
173 section 2.4.

174

175 **3 Results and discussion**

176 3.1 Characterization of the drug-loaded aerogel microspheres

177 Aerogel microspheres were obtained by means of an emulsion-gelation method coupled to
178 supercritical drying, in the form of a powder constituted by non-agglomerated particles of mean
179 particle size in the range of 100 to 550 μm (Table 1) depending on the nature of the precursor.
180 Alginate and silica aerogel microspheres showed the lowest mean particle diameters. Particle sizes of
181 aerogel microspheres are mainly influenced by the gelation process and chemical composition (i.e.
182 gelation mechanism, cross-linker, viscosity of the emulsion, emulsifier used or stirring rate among
183 others) (García-González, Alnaief & Smirnova, 2011; García-González, Uy, Alnaief & Smirnova,
184 2012). Resulting aerogels showed low density ($\rho < 0.25 \text{ g/cm}^3$), high porosity ($\varepsilon > 85\%$) and high
185 specific surfaces area ($> 100 \text{ m}^2/\text{g}$, Table 1). Specific surface areas of pectin and alginate aerogels were
186 much higher than those of starch aerogels, but still significantly lower than that of silica aerogel. The
187 values for the specific surface area depend on the three-dimensional structure of the gel, which is
188 mainly governed by the degree of crosslinking of the gel (García-González, Alnaief & Smirnova,
189 2011). For starch aerogels, higher specific surface area is accordingly obtained by using a high
190 amylose content starch source that provides a less-ordered amorphous network structure, a gelation
191 temperature high enough to promote full disruption of the original starch granules and a low
192 retrogradation temperature favoring crystal nucleation rather than crystal growth (García-González &
193 Smirnova, 2013; Mehling, Smirnova, Guenther & Neubert, 2009). For Ca-alginate aerogels, an
194 increase in the calcium cross-linker salt concentration and in the alginate concentration leads to an
195 increased degree of cross-linking (egg-box model) and a subsequent increase in the specific surface
196 area obtained (Alnaief, Alzaitoun, García-González & Smirnova, 2011). For pectin aerogels, the
197 choice of the pectin source (with different degrees of esterification) and the gelation mechanism
198 (acidic, thermal or ionic gelation mechanism) largely influences the physical stability and specific
199 surface area of the aerogel (García-González, Carenza, Zeng, Smirnova & Roig, 2012; White, Budarin
200 & Clark, 2010).

201 SEM images of aerogel microspheres before and after impregnation with ketoprofen and benzoic acid
202 (Fig. 2) revealed no significant morphological changes in the matrix due to drug impregnation via

203 scCO₂ technology. High magnifications (Fig. 2,right) evidenced that drug loading did not affect the
204 nanoporous structure of matrices and no sharp edges typical for drug crystals were observed in any of
205 the ketoprofen or benzoic acid-loaded microspheres.

206 Production of the aerogel microspheres through emulsion-gelation did not influence the crystallinity of
207 the polysaccharide matrix, as confirmed by XRD analysis (Fig. 3). Moreover, the absence of the
208 characteristic peaks of ketoprofen (6.4, 18.2 and 23.2° 2θ) and benzoic acid (8.2° 2θ) in the respective
209 drug-loaded aerogel microspheres confirmed the absence of drug crystals in the aerogels. Conversely,
210 peaks corresponding to benzoic acid and ketoprofen crystals were observed for the physical mixtures
211 of each drug with ground powders of starch microspheres (Figs. 3d and 3g) prepared at similar mass
212 ratio as in the drug-impregnated aerogels; thus it was discarded that the XRD sensitivity was not high
213 enough to detect the presence of drug crystals in the drug-loaded aerogels. **Moreover, control trials**
214 **with the drugs processed at the same supercritical operating conditions used for drug impregnation in**
215 **aerogels show neither change in the XRD-pattern with respect to the raw drug nor the appearance of**
216 **any polymorph of the drug. Amorphisation of the drug loaded in the aerogel matrices should be linked**
217 **to the impregnation process itself.**

218 Contact angle measurement test by applying a water droplet to the aerogel microsphere surfaces was
219 used to determine their hydrophilicity/hydrophobicity as well as to get an indication of the aerogel
220 structure integrity behavior and morphology in presence of water. Due to the porous structure of
221 aerogel microspheres, water droplet was absorbed into the network and disappeared in few
222 milliseconds (Fig. 4). Afterwards, polymer erosion occurred for aerogels and the structure collapsed at
223 different velocities and intensities depending on the type of polymeric material. Starch microspheres
224 showed more resistance against hydration, whereas silica and pectin microspheres were prone to a
225 rapid collapse of the porous network once in contact to water. Any conclusion can be poorly derived
226 for alginate microspheres based on the sensitivity of the measurement method due to the small
227 diameter of the aerogel, although a sudden material collapse seems to appear just after water
228 deposition (Fig. 4-bottom center). The observed pore collapse is a physical degradation taking place
229 due to mechanical stresses: upon contact with an aqueous medium and due to the liquid/air interfacial
230 surface tension, the open nanoporous structure of hydrophilic aerogels allows the penetration of water

231 therein resulting in large capillary forces taking place and inducing compression stresses enough to
232 collapse the aerogel network (Hüsing & Schubert, 1998). In general, a more rapid matrix collapse may
233 accelerate drug release (Kim & Pack, 2006; Mathiowitz et al., 1997; Shen, Kipper, Dziadul, Lim &
234 Narasimhan, 2002; Spenlehauer, Vert, Benoit & Boddaert, 1989). Even though erosion is not the only
235 factor influencing the drug release process, this experiment may shed light on detection of erosion
236 during the drug dissolution process and to what extent it may play a role in releasing drug molecules
237 into the medium.

238 3.2 Drug entrapment efficiency

239 Ketoprofen and benzoic acid were loaded into the aerogels by supercritical impregnation. The
240 preference for supercritical impregnation of aerogels rather than other drug loading techniques (e.g.,
241 before gelation or during solvent exchange) stems from the poor solubility in water and good
242 solubility in scCO₂ of these drugs, thus leading to higher drug loadings of the aerogels in the former
243 case (García-González, Alnaief & Smirnova, 2011). As a rule-of-thumb, the highest drug loading
244 capacities of aerogels are usually correlated with the largest specific surface area. Accordingly, silica
245 aerogel microparticles had the highest drug loading for both ketoprofen and benzoic acid, among the
246 four types of microspheres tested (Table 1). Nevertheless, drug loading of alginate, starch and pectin
247 microparticles did not obey the same tendency and was also dependent on the drug to be loaded.
248 Moreover, starch aerogel microspheres were more prone to adsorb drug molecules since they
249 presented the highest specific loading capacity for ketoprofen among the aerogels tested. These
250 findings suggest that, apart from specific surface area, other factors such as surface chemistry and
251 API-aerogel carrier interaction may also influence the drug adsorption when using different sources of
252 polymer matrices and thus determining the percentage of drug loading in the aerogel. Specific loading
253 values for ketoprofen were lower than those expected for a monolayer coverage ($1.7\text{-}2.1 \times 10^{-3} \text{ g/m}^2$) in
254 all cases. Ketoprofen adsorption coverages in the aerogels below the monolayer coverage might be
255 explained by surface hydroxyl group density in the aerogel and the competitive physisorption of CO₂
256 molecules during the supercritical fluid-assisted impregnation process (Gorle, Smirnova & Arlt, 2010;
257 Tripp & Combes, 1998). Ketoprofen interacts with hydroxyl groups in the aerogel by hydrogen
258 bonding through the carbonyl and carboxyl groups present in this drug molecule (Lozano & Martínez,

259 2006). The density of OH groups in starch aerogels is estimated to be 4–10 times higher than that of
260 silica aerogels (García-González, Camino-Rey, Alnaief, Zetzl & Smirnova, 2012). Starch is also the
261 only polysaccharide used in this study without acid groups in its molecular structure, thus avoiding the
262 electrostatic repulsions of the drug molecules that may take place for the other polysaccharides.
263 Stronger chemical interaction between the adsorbed drug molecules and the starch matrices might be
264 thus behind the observed behavior of high ketoprofen specific loadings compared to the other aerogels.
265 Moreover, starch (mainly amylose) can adopt helical structures with a hydrophobic cavity able to host
266 drugs, such as benzoic acid (Uchino, Tozuka, Oguchi & Yamamoto, 2002) and recently reported for
267 ketoprofen (Messner, Häusler & Loftsson, 2012), leading to the formation of inclusion complexes,
268 which should contribute to greater drug uptakes. Namely, benzoic acid was reported to induce changes
269 in the amylose helical structure to form inclusion complexes of amylose with the drug by using the
270 sealed-heating process (Uchino, Tozuka, Oguchi & Yamamoto, 2002). This processing technique
271 stems from the ability of evaporation of the drug at a given temperature to access the amylose helical
272 structure and form the inclusion complex, observed through the appearance of XRD peaks at 6.8, 12.9,
273 18.0° 2 θ in the case of benzoic acid. Analogously, the supercritical impregnation process might be a
274 low-temperature alternative to the sealed-heating process able to incorporate the benzoic acid in the
275 helical amylose cavities due to the inherently low viscosity and high diffusivity of the supercritical
276 solutions containing the drug. Evidences of inclusion formation by XRD in the benzoic acid-loaded
277 starch aerogel cannot be confirmed in Fig 3e due to the low degree of crystallinity of the sample
278 arising from its high amylose content and low hydration (Cheetham & Tao, 1998). Nevertheless, the
279 presence of an incipient peak at 18.0° 2 θ (as indicated by an asterisk in the figure), main diffraction
280 peak of benzoic acid–7₁-helix structure amylose inclusion complex, seems to indicate the formation of
281 an inclusion complex between benzoic acid and the starch (amylose) matrix. For the other aerogels
282 loaded with benzoic acid, the specific loadings lies in the region of $2-4 \times 10^{-4}$ g benzoic acid/m² where
283 the absence of drug crystals was previously reported (Gorle, Smirnova & Arlt, 2010). Overall, benzoic
284 acid loading and drug entrapment efficiency values were much higher than ketoprofen loading ones
285 regardless of the polymer matrix considered. This can be explained by the much lower molecular
286 weight of benzoic acid (122.12 g/mol for benzoic acid and 254.28 g/mol for ketoprofen) as well as the

287 configuration of benzoic acid molecule (flat molecule: 0.50 nm×0.72 nm) compared to ketoprofen
288 molecule (3D-molecule: 0.50 nm×1.22 nm×0.45nm).

289 3.3 Release of ketoprofen and benzoic acid

290 For drug delivery systems composed of biodegradable and water-soluble organic materials, three
291 important factors –diffusion, dissolution and polymeric matrix erosion upon degradation – can be
292 involved in the drug release process. *In vitro* cumulative release profiles of ketoprofen from different
293 types of polysaccharide aerogel microspheres in pH 6.8 buffer solution are shown in Fig. 5. Similar
294 patterns were observed in all cases, i.e. an initially fast dissolution rate during the first two hours was
295 followed by a sustained release up to reaching a plateau. During these two hours, alginate and pectin
296 microspheres released *ca.* 80% of the total ketoprofen impregnated, whereas starch microspheres
297 released only 54.5%. The faster release rate of alginate and pectin microspheres in comparison to
298 starch ones may stem from the matrix interaction with the aqueous medium and also from the weaker
299 drug-matrix interactions. Pectin (Vaclavik & Christian, 2007) and alginate (Berger, Ludwig & Wielich,
300 1953) are proved to be highly hydrophilic leading to rapid collapse of the aerogel porous network in
301 aqueous medium; thus, amorphous drug molecules can be released to the buffer solution. Besides, the
302 different drug release rate from alginate and pectin microspheres in comparison to that from starch
303 microparticles may stem from the higher specific surface areas of the former ones (Table 1). The
304 slightly incomplete release observed for pectin microspheres (82.02 % at 1440 min) compared to
305 alginate ones, can be explained by the combination of lower specific surface area, larger particle size
306 of pectin and drug-matrix chemical interactions.

307 The release of ketoprofen contained in silica aerogel microspheres, a non-biodegradable polymeric
308 matrix, showed a prompt drug release (60% in the first 60 min) followed by a slow release of 2%
309 within the next 23 h (Fig. 5). The high specific surface area of silica aerogels facilitates the release of
310 larger amounts of ketoprofen as a burst compared to the release of the drug from the polysaccharide
311 aerogels. The non-degradability of silica under the release conditions coupled to the dramatic blockage
312 of the drug in the inner core of the silica microspheres due to the porous network collapse observed for
313 these aerogels once in contact with water may hinder the release by diffusion of the remaining
314 ketoprofen to the surrounding medium.

315 Three mathematical models (Korsmeyer-Peppas model (Eq. (1)), first-order model (Eq. (2)) and
 316 Gallagher-Corrigan model (Eq(3))) emphasizing on different release phenomena were used to fit the
 317 drug release profile with the aid of Origin 8 software (Balcerzak & Mucha, 2010; Dash, Murthy, Nath
 318 & Chowdhury, 2010):

$$319 \quad F = k \cdot t^n \quad \text{Eq. (1)}$$

$$320 \quad F = F_{\max} [1 - \exp(-k_1 \cdot t)] \quad \text{Eq. (2)}$$

$$321 \quad F = F_{\max} [1 - \exp(-k_1 t)] + (F_{\max} - F_B) \left[\frac{\exp(k_2 \cdot t - k_2 \cdot t_{2\max})}{1 + \exp(k_2 \cdot t - k_2 \cdot t_{2\max})} \right] \quad \text{Eq. (3)}$$

322 where F is the fraction (in percentage) of drug released at a certain time t , F_{\max} stands for the
 323 maximum fraction of drug released during the total time period, and k_1 and k_2 are the first order kinetic
 324 coefficient and the kinetic coefficient for the second stage in min^{-1} , respectively. In Eq. (1) n denotes
 325 the release exponent, while F_B in Eq. (3) indicates the drug fraction released in the first release stage.
 326 The criterion of only validating a correlation when $R^2 > 0.98$ was adopted.

327 The Gallagher-Corrigan model fitted ketoprofen release from pectin aerogel microparticles ($R^2 > 0.999$,
 328 Table 2). This model fitting denotes a two-phase drug release profile, incorporating an initial burst
 329 release (phase I) followed by a slower polymeric matrix bulk degradation (erosion)-controlled release
 330 phase (phase II) (Gallagher & Corrigan, 2000). During the phase I, a fraction of 25.0% of the total
 331 non-crystalline drug (F_B) easily dissolved once the matrix comes into contact with the surrounding
 332 aqueous medium, which meant that this fraction of drug was the most accessible one, being only
 333 physically adsorbed to the external surface or in large pores of the aerogel matrix. Ketoprofen fraction
 334 entrapped in the pectin microspheres represents 56.6% of drug molecules ($F_{\max} - F_B$) and is only
 335 released out in the phase II after pectin aerogel matrix degradation. Moreover, pectin microspheres
 336 provided a rapid release profile with a significantly higher simulated degradation kinetic coefficient
 337 ($k_2 = 0.093 \text{ min}^{-1}$) compared to diffusion kinetic coefficient ($k_1 = 0.023 \text{ min}^{-1}$). This suggests a rapid bulk
 338 degradation process, which is attributed to the high hydrophilicity and chemical instability of pectin
 339 aerogels in pH 6.8 buffer solution.

340 For ketoprofen release from alginate aerogel microspheres, both Korsmeyer-Peppas and Gallagher-
 341 Corrigan models showed comparable fitting wellness ($R^2 > 0.99$, Table 2). In this case, the diffusion

342 kinetic coefficient ($k_1=0.026 \text{ min}^{-1}$) was higher than the degradation kinetic coefficient ($k_2=0.010 \text{ min}^{-1}$), suggesting that drug release is likely diffusion-controlled assisted by polysaccharide erosion. The n
343 value of Korsmeyer-Peppas model below 0.43, an extreme value for spherical dosage forms (Ritger &
344 Peppas, 1987), suggests the initial diffusion process of ketoprofen following the Fickian diffusion
345 mechanism and endorses the diffusion-control hypothesis.

347 First order kinetics was the best model fitting ketoprofen release from starch aerogel microspheres
348 ($R^2=0.987$) (Table 2). The wellness of the first order model fitting suggests that drug dissolution from
349 starch aerogel microspheres is the governing factor of ketoprofen release where the solid matrix
350 morphology remains intact during the dissolution process. Gallagher Corrigan model, with an
351 excellent correlation and a significantly low k_2 value, and Korsmeyer-Peppas model, with a n -value of
352 0.40, endorsed a first-order model following the Fickian release. A prompt drug release from starch
353 microspheres resulted in 53% of the total loaded drug dissolved in neutral medium in the first 60 min,
354 followed by an increment of 3% in release rate within 24 h. Drug remaining in the starch aerogel may
355 be forming an insoluble inclusion complex in the aerogel matrix.

356 Release behavior of ketoprofen from aerogel microspheres was also investigated at acidic conditions
357 (pH 1.2, gastric pH conditions), in order to determine their potential to promote fast release in the
358 gastric environment (Figs. 6 and 7). Ketoprofen, as well many other non-steroidal anti-inflammatory
359 drugs (NSAIDs) is characterized by a pH-dependent solubility profile due to their weak acid character
360 (Sheng, Kasim, Chandrasekharan & Amidon, 2006). Thus, ketoprofen crystals (pKa 4.4-4.8) exhibit
361 low solubility and dissolution rate under acidic conditions. Moreover, cross-linked pectin and alginate
362 microspheres are resistant to acidic conditions and are not able to dissolve in aqueous media, likely
363 influencing the release behavior of the drug incorporated to these carriers (Del Gaudio, Colombo,
364 Colombo, Russo & Sonvico, 2005; Sriamornsak, 2003). The kinetic analysis of the ketoprofen release
365 from alginate and pectin microsphere aerogels is summarized in Table 3.

366 In contrast to drug release profiles at pH 6.8, alginate microspheres accelerated ketoprofen release at
367 simulated gastric pH conditions (Fig. 6), which is consistent with previous reports (Radin, Chen &
368 Ducheyne, 2009). pK_a values of both alginate (1.5-3.5) and ketoprofen (4.4-4.8) are in the 1.2-6.8 pH
369 range leading to different ionic forms of the drug and the carrier in PBS and simulated gastric fluid

370 conditions. Besides, non-crystalline drug molecules located in aerogel microspheres may require much
371 less time for dissolution than pure ketoprofen crystals (Sheng, Kasim, Chandrasekharan & Amidon,
372 2006). As denoted by the Korsmeyer-Peppas model, ketoprofen release from alginate aerogel
373 microspheres at pH 1.2 mainly follows a diffusion profile similar to that obtained at pH 6.8, but with a
374 higher value of the diffusion coefficient at pH 1.2.

375 Ketoprofen release from pectin microspheres at pH 1.2 (Fig. 7) was slower than at pH 6.8 during the
376 first 2 h, although again faster than the profile recorded for the free crystalline drug. After 2 h, drug
377 release rate at acidic conditions exceeded the release rate at neutral conditions, finally reaching 98%
378 drug released (compared to 80% released at pH 6.8). This finding can be well explained by the pectin
379 matrix properties. The initial slower release rate at pH 1.2 is due to the lower swelling ratio of the
380 pectin matrix at acidic conditions, due to the high proportion of unionized carboxylic groups. After a
381 certain time period, the swelling effect decreases likely due to matrix degradation (Sriamornsak, 2003)
382 and drug-pectin interaction should govern the drug release. Due to the small particle size of the
383 aerogel microspheres, swelling and water uptake studies were not able to be carried out to confirm this
384 effect, in contrast to other studies with small aerogel monoliths or gel beads both falling in the size
385 range of few millimeters (Betz, García-González, Subrahmanyam, Smirnova & Kulozik, 2012; Del
386 Gaudio, Colombo, Colombo, Russo & Sonvico, 2005), which can be both weighed or measured in a
387 straightforward way. This behavior of pectin supports the final faster release rate of ketoprofen
388 compared to that observed at pH 6.8 conditions. Accordingly, the kinetic coefficient obtained for
389 pectin aerogels at pH 1.2 ($k_2=0.113 \text{ min}^{-1}$) by the Gallagher Corrigan model is higher than that at pH
390 6.8 ($k_2=0.093 \text{ min}^{-1}$). Moreover, F_B value at pH 1.2 (86.81%) is much higher than at pH 6.8 (24.98%),
391 which is ascribed to the weaker ketoprofen-pectin interaction at pH 1.2 with respect to pH 6.8 due to
392 the change in the ionic forms of both ketoprofen and pectin at these two pH conditions.

393 The release behavior from starch aerogel microspheres of ketoprofen was compared to that of benzoic
394 acid. Both drugs have similar chemical functionalities and dissociation constant values (pK_a 4.2 for
395 benzoic acid), but different molecular weights and dimensions. Moreover, the presence benzoic acid-
396 amylose inclusion complexes may influence on the release behavior of the drug. Starch microspheres
397 loaded with benzoic acid showed the same release pattern at intestinal environment (pH 6.8) (Fig. 8)

398 as with ketoprofen, i.e. a burst release followed by a sustained release. Starch microspheres possess a
399 strong hydrophilic character and water uptake is considered to be the main controlling mechanism in
400 the initial burst period and the release period is complete within 30 min, as also reported by other
401 researchers (Atyabi, Manoochehri, Moghadam & Dinarvand, 2006). The dissolution profile of pure
402 benzoic acid was similar to that of the same drug loaded in the aerogel, but showing an initially slower
403 release rate according to the k_1 parameter from the first order release model fitting (0.160 min^{-1} for
404 benzoic acid in the starch aerogels and 0.071 min^{-1} for pure benzoic acid) likely related to the
405 amorphous state of the drug in the aerogel. However, with regard to the final benzoic acid release
406 percentage, only 63% of the total loading content from starch microspheres was released into the
407 aqueous medium whereas 90% pure benzoic acid was dissolved in the first two hours. This could be
408 the consequence of closed trapping of solute drug molecules into the starch polymeric network by
409 formation of chemical bonds (carboxylic group of benzoic acid with hydroxyl group of starch matrix)
410 (Vyas & Jain, 1992) and the presence of amylose-benzoic acid inclusion complexes. Release of
411 benzoic from starch aerogel microspheres was faster than that of ketoprofen with the same aerogel
412 carrier. The difference in dissolution behavior between ketoprofen and benzoic acid may stem from the
413 smaller dimension of benzoic acid, which makes it easier diffusing from starch polymeric network,
414 and different drug-matrix interactions.

415 **4 Conclusions**

416 Different types of biodegradable polysaccharide-based aerogel microspheres including alginate, pectin
417 and starch were evaluated regarding their feasibility to be used as drug carriers for life science
418 applications. The processing method used provides a suitable morphology of the micronized carrier
419 with improved product reproducibility, an amorphous drug-loaded delivery system with loadings in
420 the range of 11-24 wt.%, and an expected good physicochemical stability upon storage because of the
421 dry solid format of the formulation. Drug loading capacity was dependent on the specific surface area
422 and surface chemistry of the aerogels as well as on the drug-aerogel matrix chemical interaction.
423 Material hydrophilicity tests with a high-speed camera were suitable to unveil different erosion
424 mechanism of the aerogel in contact with aqueous medium depending on the aerogel origin (fast
425 erosion for pectin and alginate and slow erosion for starch aerogels). Release of ketoprofen from

426 alginate and pectin aerogel particles was sensitive to pH values of the aqueous medium (pH 1.2 or 6.8).
427 Namely, alginate aerogel microspheres showed accelerated drug release behavior at simulated gastric
428 pH conditions favoring ketoprofen dissolution at this point. The release profiles of the polysaccharide
429 aerogel microspheres are governed by one or two release mechanisms depending on the aerogel
430 matrix. This different drug release behavior observed for polysaccharide aerogel matrices opens up the
431 possibility of using these nanostructured materials as carriers for developing tailor-made drug release
432 profiles for oral applications.

433

434 **Acknowledgments**

435 C.A. García-González acknowledges the Spanish Ministry of Science and Innovation (MICINN) for
436 the financial support through the Juan de la Cierva Fellowship Programme (Grant N° JCI-2012-12705).
437 The work was partially funded by the Spanish Government (MICINN, SAF2011-22771) and the
438 European Commission (FEDER funds). The authors also thank Krüss GmbH (Hamburg, Germany)
439 for providing the usage of DSA 100 M to carry out the contact angle measurements, and Roquette
440 Frères (Dr. O. Häusler) for the supply of the corn starch.

441 **Appendix A. Supplementary data**

442 Supplementary data associated with this article can be found in the online version.

443 **References**

- 444 Alnaief, M., Alzaitoun, M. A., García-González, C. A., & Smirnova, I. (2011). Preparation of
445 biodegradable nanoporous microspherical aerogel based on alginate. *Carbohydrate Polymers*, *84*(3),
446 1011-1018.
- 447 Alnaief, M., & Smirnova, I. (2011). In situ production of spherical aerogel microparticles. *The Journal*
448 *of Supercritical Fluids*, *55*(3), 1118-1123.
- 449 Alvarez-Lorenzo, C., Blanco-Fernandez, B., Puga, A. M., & Concheiro, A. (2013). Crosslinked ionic
450 polysaccharides for stimuli-sensitive drug delivery. *Advanced Drug Delivery Reviews*, *65*(9), 1148-
451 1171.
- 452 Atyabi, F., Manoochehri, S., Moghadam, S., & Dinarvand, R. (2006). Cross-linked starch
453 microspheres: Effect of cross-linking condition on the microsphere characteristics. *Archives of*
454 *Pharmaceutical Research*, *29*(12), 1179-1186.
- 455 Balcerzak, J., & Mucha, M. (2010). Analysis of model drug release kinetics from complex matrices of
456 polylactide-chitosan. *Progress on Chemistry and Application of Chitin and its Derivatives*, *15*, 117-
457 126.
- 458 Baldwin, A. D., & Kiick, K. L. (2010). Polysaccharide-modified synthetic polymeric biomaterials.
459 *Peptide Science*, *94*(1), 128-140.
- 460 Berg, A., Droege, M. W., Fellmann, J. D., Klaveness, J., & Rongved, P. (1995). Medical use of
461 organic aerogels and biodegradable organic aerogels. (Vol. WO1995001165 A1). Great Britain.
- 462 Berger, F. M., Ludwig, B. J., & Wielich, K. H. (1953). The hydrophilic and acid binding properties of
463 alginates. *The American Journal of Digestive Diseases*, *20*(2), 39-42.
- 464 Betz, M., García-González, C. A., Subrahmanyam, R. P., Smirnova, I., & Kulozik, U. (2012).
465 Preparation of novel whey protein-based aerogels as drug carriers for life science applications. *The*
466 *Journal of Supercritical Fluids*, *72*, 111-119.

- 467 Bhagat, S. D., Park, K.-T., Kim, Y.-H., Kim, J.-S., & Han, J.-H. (2008). A continuous production
468 process for silica aerogel powders based on sodium silicate by fluidized bed drying of wet-gel slurry.
469 *Solid State Sciences*, 10(9), 1113-1116.
- 470 Cheetham, N. W. H., & Tao, L. (1998). Variation in crystalline type with amylose content in maize
471 starch granules: an X-ray powder diffraction study. *Carbohydrate Polymers*, 36(4), 277-284.
- 472 Dash, S., Murthy, P. N., Nath, L., & Chowdhury, P. (2010). Kinetic modeling on drug release from
473 controlled drug delivery systems. *Acta Poloniae Pharmaceutica - Drug Research*, 67(3), 217-223.
- 474 Del Gaudio, P., Auriemma, G., Mencherini, T., Porta, G. D., Reverchon, E., & Aquino, R. P. (2013).
475 Design of alginate-based aerogel for nonsteroidal anti-inflammatory drugs controlled delivery systems
476 using prilling and supercritical-assisted drying. *Journal of Pharmaceutical Sciences*, 102(1), 185-194.
- 477 Del Gaudio, P., Colombo, P., Colombo, G., Russo, P., & Sonvico, F. (2005). Mechanisms of
478 formation and disintegration of alginate beads obtained by prilling. *International Journal of*
479 *Pharmaceutics*, 302(1-2), 1-9.
- 480 Dumitriu, S. (2012). *Polysaccharides: Structural diversity and functional versatility, Second Edition*.
481 New York, NY, USA: CRC Press.
- 482 Gallagher, K. M., & Corrigan, O. I. (2000). Mechanistic aspects of the release of levamisole
483 hydrochloride from biodegradable polymers. *Journal of Controlled Release*, 69(2), 261-272.
- 484 García-González, C. A., Alnaief, M., & Smirnova, I. (2011). Polysaccharide-based aerogels -
485 Promising biodegradable carriers for drug delivery systems. *Carbohydrate Polymers*, 86(4), 1425-
486 1438.
- 487 García-González, C. A., Argemí, A., Sousa, A. R. S. d., Duarte, C. M. M., Saurina, J., & Domingo, C.
488 (2010). Encapsulation efficiency of solid lipid hybrid particles prepared using the PGSS[®] technique
489 and loaded with different polarity active agents. *The Journal of Supercritical Fluids*, 54(3), 342-347.
- 490 García-González, C. A., Camino-Rey, M. C., Alnaief, M., Zetzl, C., & Smirnova, I. (2012).
491 Supercritical drying of aerogels using CO₂: Effect of extraction time on the end material textural
492 properties. *The Journal of Supercritical Fluids*, 66, 297-306.
- 493 García-González, C. A., Carezza, E., Zeng, M., Smirnova, I., & Roig, A. (2012). Design of
494 biocompatible magnetic pectin aerogel monoliths and microspheres. *RSC Advances*, 2(26), 9816-9823.
- 495 García-González, C. A., & Smirnova, I. (2013). Use of supercritical fluid technology for the
496 production of tailor-made aerogel particles for delivery systems. *The Journal of Supercritical Fluids*,
497 79, 152-158.
- 498 García-González, C. A., Uy, J. J., Alnaief, M., & Smirnova, I. (2012). Preparation of tailor-made
499 starch-based aerogel microspheres by the emulsion-gelation method. *Carbohydrate Polymers*, 88(4),
500 1378-1386.
- 501 Gorle, B. S. K., Smirnova, I., & Arlt, W. (2010). Adsorptive crystallization of benzoic acid in aerogels
502 from supercritical solutions. *The Journal of Supercritical Fluids*, 52(3), 249-257.
- 503 Hong, S. K., Yoon, M. Y., & Hwang, H. J. (2011). Fabrication of Spherical Silica Aerogel Granules
504 from Water Glass by Ambient Pressure Drying. *Journal of the American Ceramic Society*, 94(10),
505 3198-3201.

- 506 Hüsing, N., & Schubert, U. (1998). Aerogels—Airy Materials: Chemistry, Structure, and Properties.
507 *Angewandte Chemie International Edition*, 37(1-2), 22-45.
- 508 Jin, J., Zhong, C., Zhang, Z., & Li, Y. (2004). Solubilities of benzoic acid in supercritical CO₂ with
509 mixed cosolvent. *Fluid Phase Equilibria*, 226, 9-13.
- 510 Kayser, H., Müller, C. R., García-González, C. A., Smirnova, I., Leitner, W., & Domínguez de María,
511 P. (2012). Dried chitosan-gels as organocatalysts for the production of biomass-derived platform
512 chemicals. *Applied Catalysis A: General*, 445-446, 180-186.
- 513 Kim, K. K., & Pack, D. W. (2006). Microspheres for drug delivery. *BioMEMS and Biomedical*
514 *Nanotechnology* (pp. 19-50). New York, NY, USA: Springer US.
- 515 Lozano, H. R., & Martínez, F. (2006). Thermodynamics of partitioning and solvation of ketoprofen in
516 some organic solvent/buffer and liposome systems. *Brazilian Journal of Pharmaceutical Sciences*,
517 42(4), 601-613.
- 518 Mathiowitz, E., Jacob, J. S., Jong, Y. S., Carino, G. P., Chickering, D. E., Chaturvedi, P., Santos, C. A.,
519 Vijayaraghavan, K., Montgomery, S., Bassett, M., & Morrell, C. (1997). Biologically erodable
520 microspheres as potential oral drug delivery systems. *Nature*, 386(6623), 410-414.
- 521 Mehling, T., Smirnova, I., Guenther, U., & Neubert, R. H. H. (2009). Polysaccharide-based aerogels
522 as drug carriers. *Journal of Non-Crystalline Solids*, 355(50-51), 2472-2479.
- 523 Messner, M., Häusler, O., & Loftsson, T. (2012). Solution enhancement of drug substances using
524 soluble amylose. *Proceedings of PBP 8th World Meeting on Pharmaceutics, Biopharmaceutics and*
525 *Pharmaceutical Technology*. Istanbul (Turkey).
- 526 O'Donnell, P. B., & McGinity, J. W. (1997). Preparation of microspheres by the solvent evaporation
527 technique. *Advanced Drug Delivery Reviews*, 28(1), 25-42.
- 528 Pose-Vilarnovo, B., Rodríguez-Tenreiro, C., Rosa dos Santos, J. F., Vázquez-Doval, J., Concheiro, A.,
529 Alvarez-Lorenzo, C., & Torres-Labandeira, J. J. (2004). Modulating drug release with cyclodextrins in
530 hydroxypropyl methylcellulose gels and tablets. *Journal of Controlled Release*, 94(2-3), 351-363.
- 531 Radin, S., Chen, T., & Ducheyne, P. (2009). The controlled release of drugs from emulsified, sol gel
532 processed silica microspheres. *Biomaterials*, 30(5), 850-858.
- 533 Ritger, P. L., & Peppas, N. A. (1987). A simple equation for description of solute release I. Fickian
534 and non-fickian release from non-swellable devices in the form of slabs, spheres, cylinders or discs.
535 *Journal of Controlled Release*, 5(1), 23-36.
- 536 Rothstein, S. N., Federspiel, W. J., & Little, S. R. (2009). A unified mathematical model for the
537 prediction of controlled release from surface and bulk eroding polymer matrices. *Biomaterials*, 30(8),
538 1657-1664.
- 539 Sarawade, P. B., Kim, J.-K., Hilonga, A., Quang, D. V., Jeon, S. J., & Kim, H. T. (2011). Synthesis of
540 sodium silicate-based hydrophilic silica aerogel beads with superior properties: Effect of heat-
541 treatment. *Journal of Non-Crystalline Solids*, 357(10), 2156-2162.
- 542 Shen, E., Kipper, M. J., Dziadul, B., Lim, M.-K., & Narasimhan, B. (2002). Mechanistic relationships
543 between polymer microstructure and drug release kinetics in bioerodible polyanhydrides. *Journal of*
544 *Controlled Release*, 82(1), 115-125.

- 545 Sheng, J. J., Kasim, N. A., Chandrasekharan, R., & Amidon, G. L. (2006). Solubilization and
546 dissolution of insoluble weak acid, ketoprofen: Effects of pH combined with surfactant. *European*
547 *Journal of Pharmaceutical Sciences*, 29(3-4), 306-314.
- 548 Smirnova, I., Suttiruengwong, S., & Arlt, W. (2004). Feasibility study of hydrophilic and hydrophobic
549 silica aerogels as drug delivery systems. *Journal of Non-Crystalline Solids*, 350, 54-60.
- 550 Spenlehauer, G., Vert, M., Benoit, J. P., & Boddaert, A. (1989). In vitro and In vivo degradation of
551 poly(D,L lactide/glycolide) type microspheres made by solvent evaporation method. *Biomaterials*,
552 10(8), 557-563.
- 553 Sriamornsak, P. (2003). Chemistry of pectin and its pharmaceutical uses: A review. *Silpakorn*
554 *University Journal Of Social Sciences, Humanities, and Arts*, 3(1-2), 206–228.
- 555 Stassi, A., Bettini, R., Gazzaniga, A., Giordano, F., & Schiraldi, A. (2000). Assessment of solubility of
556 ketoprofen and vanillic acid in supercritical CO₂ under dynamic conditions. *Journal of Chemical &*
557 *Engineering Data*, 45(2), 161-165.
- 558 Tripp, C. P., & Combes, J. R. (1998). Chemical Modification of Metal Oxide Surfaces in Supercritical
559 CO₂: The Interaction of Supercritical CO₂ with the Adsorbed Water Layer and the Surface Hydroxyl
560 Groups of a Silica Surface. *Langmuir*, 14(26), 7348-7352.
- 561 Uchino, T., Tozuka, Y., Oguchi, T., & Yamamoto, K. (2002). Inclusion compound formation of
562 amylose by sealed-heating with salicylic acid analogues. *Journal of inclusion phenomena and*
563 *macrocylic chemistry*, 43(1-2), 31-36.
- 564 Ulker, Z., & Erkey, C. (2014). An emerging platform for drug delivery: Aerogel based systems.
565 *Journal of Controlled Release*, 177, 51-63.
- 566 Vaclavik, V., & Christian, E. W. (2007). *Essentials of food science*. New York, NY, USA: Springer.
- 567 Valentin, R., Molvinger, K., Quignard, F., & Di Renzo, F. (2005). Methods to analyse the texture of
568 alginate aerogel microspheres. *Macromolecular Symposia*, 222(1), 93-102.
- 569 Veronovski, A., Knez, Ž., & Novak, Z. (2013). Preparation of multi-membrane alginate aerogels used
570 for drug delivery. *The Journal of Supercritical Fluids*, 79, 209-215.
- 571 von Burkersroda, F., Schedl, L., & Göpferich, A. (2002). Why degradable polymers undergo surface
572 erosion or bulk erosion. *Biomaterials*, 23(21), 4221-4231.
- 573 Vyas, S. P., & Jain, C. P. (1992). Bioadhesive polymer-grafted starch microspheres bearing isosorbide
574 dinitrate for buccal administration. *Journal of Microencapsulation*, 9(4), 457-464.
- 575 White, R. J., Budarin, V. L., & Clark, J. H. (2010). Pectin-derived porous materials. *Chemistry – A*
576 *European Journal*, 16(4), 1326-1335.

1 **Table 1.** Physical properties and drug loading capacities for aerogel microspheres.

2

Aerogel matrix	Mean particle size [μm] ^a	Specific surface area [m^2/g] ^b	Drug loading [wt.%]		Drug entrapment efficiency [%] ^c		Specific loading [g/m^2]	
			Ketoprofen	Benzoic acid	Ketoprofen	Benzoic acid	Ketoprofen	Benzoic acid
Silica	155 \pm 7	1000 \pm 50	15.38 \pm 1.80	23.77 \pm 0.12	18.18 \pm 2.51	31.18 \pm 0.21	1.54 \times 10 ⁻⁴ \pm 1.80 \times 10 ⁻⁵	2.38 \times 10 ⁻⁴ \pm 6.50 \times 10 ⁻⁶
Alginate	116 \pm 6	524 \pm 26.4	11.83 \pm 0.61	18.92 \pm 1.32	13.42 \pm 0.78	23.33 \pm 2.01	2.26 \times 10 ⁻⁴ \pm 1.17 \times 10 ⁻⁵	3.61 \times 10 ⁻⁴ \pm 2.51 \times 10 ⁻⁵
Pectin	498 \pm 1	397 \pm 19.9	14.01 \pm 3.84	14.66 \pm 1.24	16.29 \pm 5.19	17.18 \pm 1.70	3.53 \times 10 ⁻⁴ \pm 9.66 \times 10 ⁻⁵	3.69 \times 10 ⁻⁴ \pm 3.15 \times 10 ⁻⁵
Starch	519 \pm 4	127 \pm 6.4	12.84 \pm 0.92	21.54 \pm 2.04	14.73 \pm 1.21	27.45 \pm 3.31	10.1 \times 10 ⁻⁴ \pm 7.24 \times 10 ⁻⁵	17.0 \times 10 ⁻⁴ \pm 1.61 \times 10 ⁻⁴

3 ^a Obtained prior to supercritical drying. A particle size decrease of 5-10% is expected after drying

4 ^b Obtained prior to supercritical impregnation

5 ^c Note that the remaining drug fraction is recovered in the form of dry powder in the drug cartridge and can be virtually reused for ulterior trials

6

7

8 **Table 2.** Kinetic fitting parameters of the ketoprofen release from drug-loaded aerogel microparticles in
 9 pH 6.8 buffer solution. Bold values denote the best-fit parameters for each ketoprofen-aerogel system

10

Samples	First Order			Korsmeyer-Peppas			Gallagher Corrigan					
	F _{max} (%)	k ₁ (min ⁻¹)	R ²	k(min ⁻ⁿ)	n	R ²	F _B (%)	k ₁ (min ⁻¹)	F _{max} (%)	t _{2max} (min)	k ₂ (min ⁻¹)	R ²
Pectin	81.65	0.032	0.985	3.48	0.77	0.983	24.98	0.023	81.57	22.87	0.093	0.9995
Alginate	89.99	0.028	0.923	12.86	0.40	0.998	50.74	0.026	97.08	42.70	0.010	0.998
Starch	54.90	0.075	0.987	12.18	0.40	0.953	47.96	0.068	57.21	-306.3^a	0.002	0.9991

11 ^a This unrealistic negative value of t_{2max} is likely a numerical incertitude problem arising from the very low value of k₂.

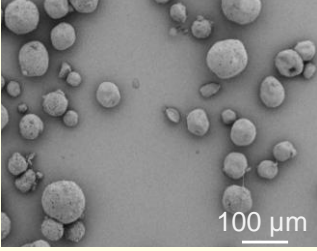
12

13 **Table 3.** Kinetic analysis of the ketoprofen release from drug-loaded aerogel microparticles in pH 1.2
 14 acidic environment. Bold values denote the best-fit parameters for each ketoprofen-aerogel system.

Samples	First Order			Korsmeyer-Peppas			Gallagher Corrigan					
	F_{max} (%)	$k_1(\text{min}^{-1})$	R^2	$k(\text{min}^{-1})$	n	R^2	F_B (%)	$k_1(\text{min}^{-1})$	F_{max} (%)	$t_{2max}(\text{min})$	$k_2(\text{min}^{-1})$	R^2
Pectin	95.51	0.014	0.996	1.38	0.93	0.991	86.81	0.015	92.90	373.76	0.113	0.997
Alginate	92.85	0.051	0.949	16.66	0.41	0.967	79.55	0.031	96.12	35.50	-0.127	0.991

15

16

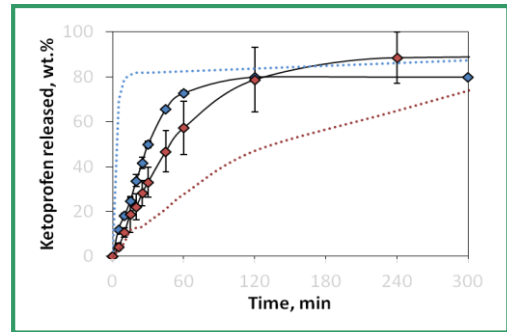


100 μm

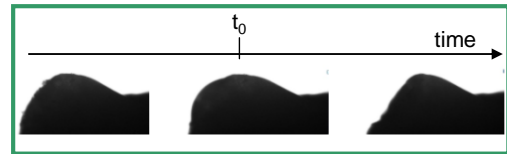
Drug-loaded polysaccharide aerogel microspheres:

- Polysaccharide:	- Drug:
Pectin	Ketoprofen
Starch	Benzoic acid
Alginate	

Drug release test +
Release modelling



Water droplet
deposition test



1 Figure Captions

2 **Fig. 1.** Schematic diagram of supercritical CO₂ impregnation equipment

3 **Fig. 2.** SEM images of (a) pure alginate aerogel microspheres, (b) ketoprofen-loaded alginate
4 microspheres, and (c) benzoic acid-loaded alginate microspheres. Scale bars represent either 2 μm (left)
5 or 200 nm (right). Alginate microspheres were herein shown as representative examples of the
6 polysaccharide aerogels studied.

7 **Fig. 3.** X-ray diffraction patterns for: ① Benzoic acid case study: (a) pure benzoic acid, (b) raw starch
8 material, (c) unloaded starch aerogel microspheres, (d) physical mixture of starch aerogel microsphere
9 with benzoic acid (15 wt.%), and (e) benzoic acid-loaded starch aerogel microspheres. ② Ketoprofen case
10 study: (f) pure ketoprofen, (g) physical mixture of starch aerogel microsphere with ketoprofen (15 wt.%),
11 and (h) ketoprofen-loaded starch aerogel microspheres. Asterisk symbol indicates the main diffraction
12 peak of benzoic acid–7₁-helix structure amylose inclusion complex.

13 **Fig. 4.** Contact angle measurement test of starch, silica, pectin and alginate aerogel microspheres (in
14 order from top to bottom). Pictures were taken before (left), at (center) and after (right) dosing a 100
15 picoliter water droplet. The stop time of the test was selected when no further structure alteration was
16 noticeable and corresponds to the so-called *after deposition test* in the figure. Projections of the contour
17 lines of the particles before water contact are added in the pictures after water contact (dashed red
18 lines) to facilitate the visual inspection of the water drop test.

19 **Fig. 5.** *In vitro* release profiles at pH 6.8 (0.1 M phosphate buffer saline solution) of ketoprofen from
20 starch (squares), alginate (diamonds), pectin (circles) and silica (pluses) aerogel microspheres (in solid
21 lines). The dissolution pattern of the same amount of free drug (triangles and dotted line) is also plotted
22 for comparison purposes.

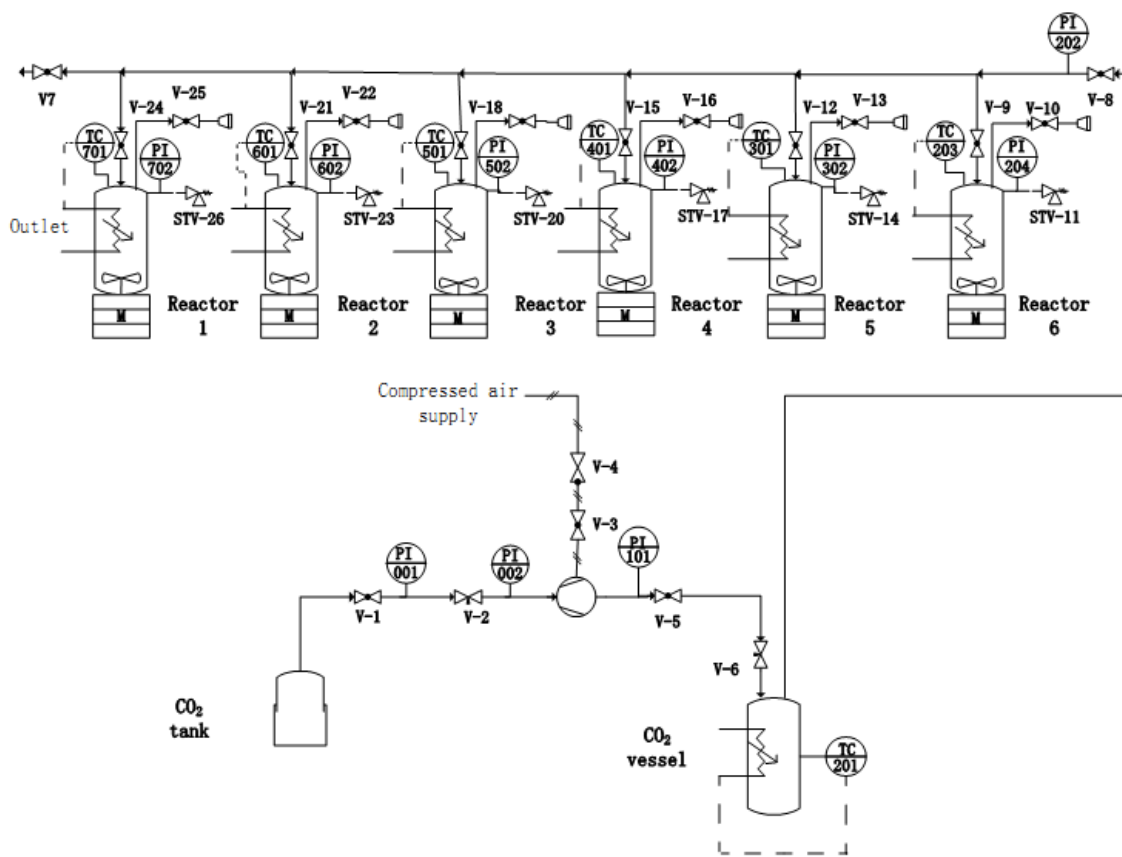
23 **Fig. 6.** *In vitro* release profiles of ketoprofen from alginate aerogel microspheres at two different pH
24 media (solid lines). Release studies of the aerogels were carried out at 37°C and pH 1.2 (0.1 N HCl, dark

25 diamonds) and 6.8 (0.1 M phosphate buffer saline solution, blank diamonds). Release profiles of the raw
26 ketoprofen (dotted lines) are also plotted for the sake of comparison (dark triangles for pH 1.2 and blank
27 triangles for pH 6.8).

28 **Fig. 7.** *In vitro* release profiles of ketoprofen from pectin aerogel microspheres at two different pH media
29 (solid lines). Release studies of the aerogels were carried out at 37°C and pH 1.2 (0.1 N HCl, dark circles)
30 and 6.8 (0.1 M phosphate buffer saline solution; blank circles). Release profiles of the raw ketoprofen
31 (dotted lines) are also plotted for the sake of comparison (dark triangles for pH 1.2 and blank triangles
32 for pH 6.8).

33 **Fig. 8.** Release profiles for starch aerogel particles loaded with benzoic acid (black squares) and
34 ketoprofen (white squares) at 37°C and pH 6.8 (0.1 M phosphate buffer saline solution) (in solid lines).
35 Release profiles of the raw ketoprofen (triangles) and benzoic acid (crosses) are also plotted (in dotted
36 lines) for the sake of comparison.

1
2
3
4
5



6
7
8
9
10
11
12
13

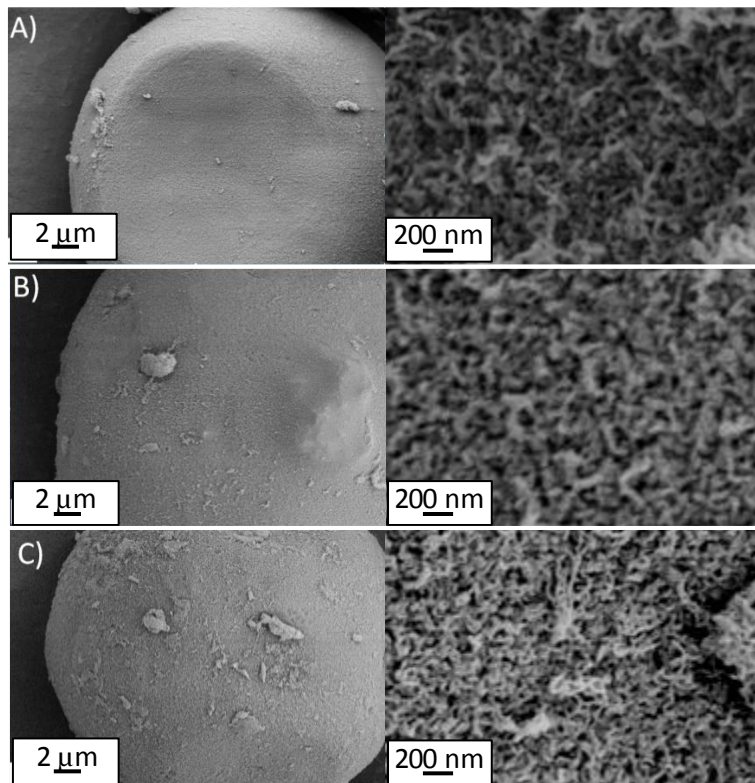
FIGURE 1

14

15

16

17



18

19

20

21

22

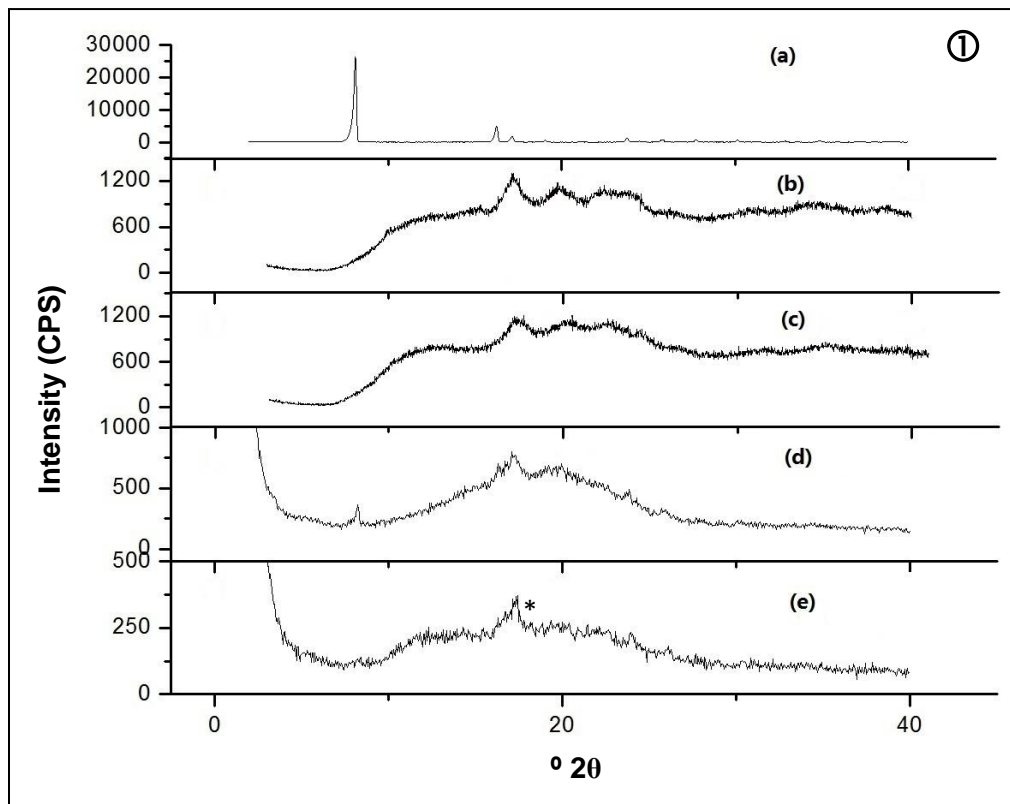
23

24

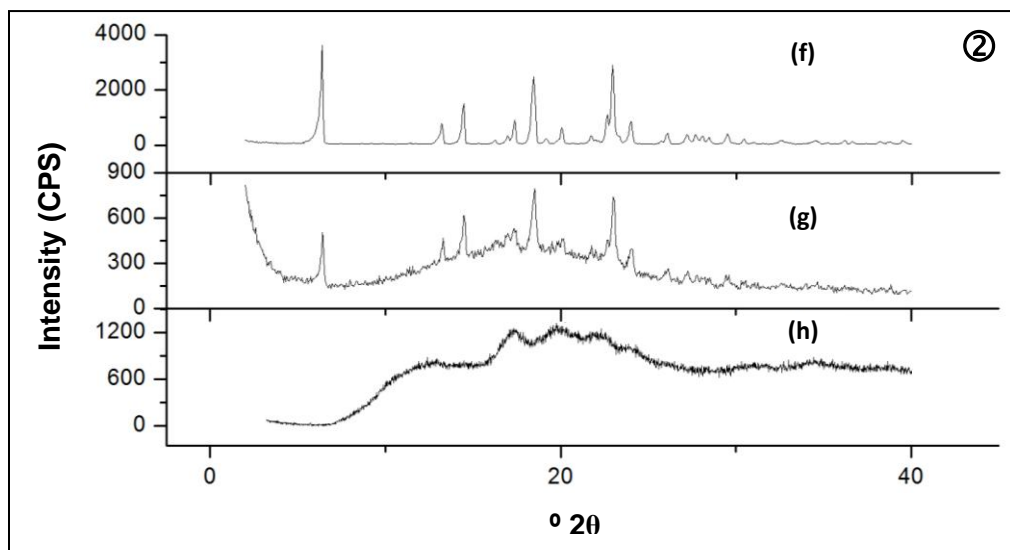
25

FIGURE 2

26



27



28

29

30

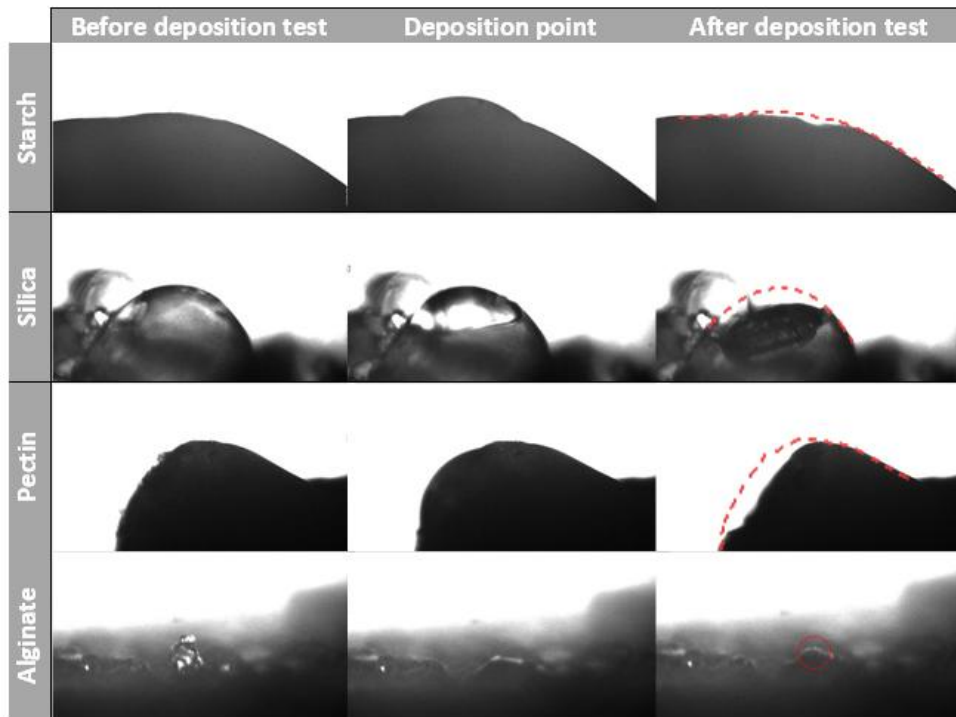
31

FIGURE 3

32

33

34



35

36

37

38

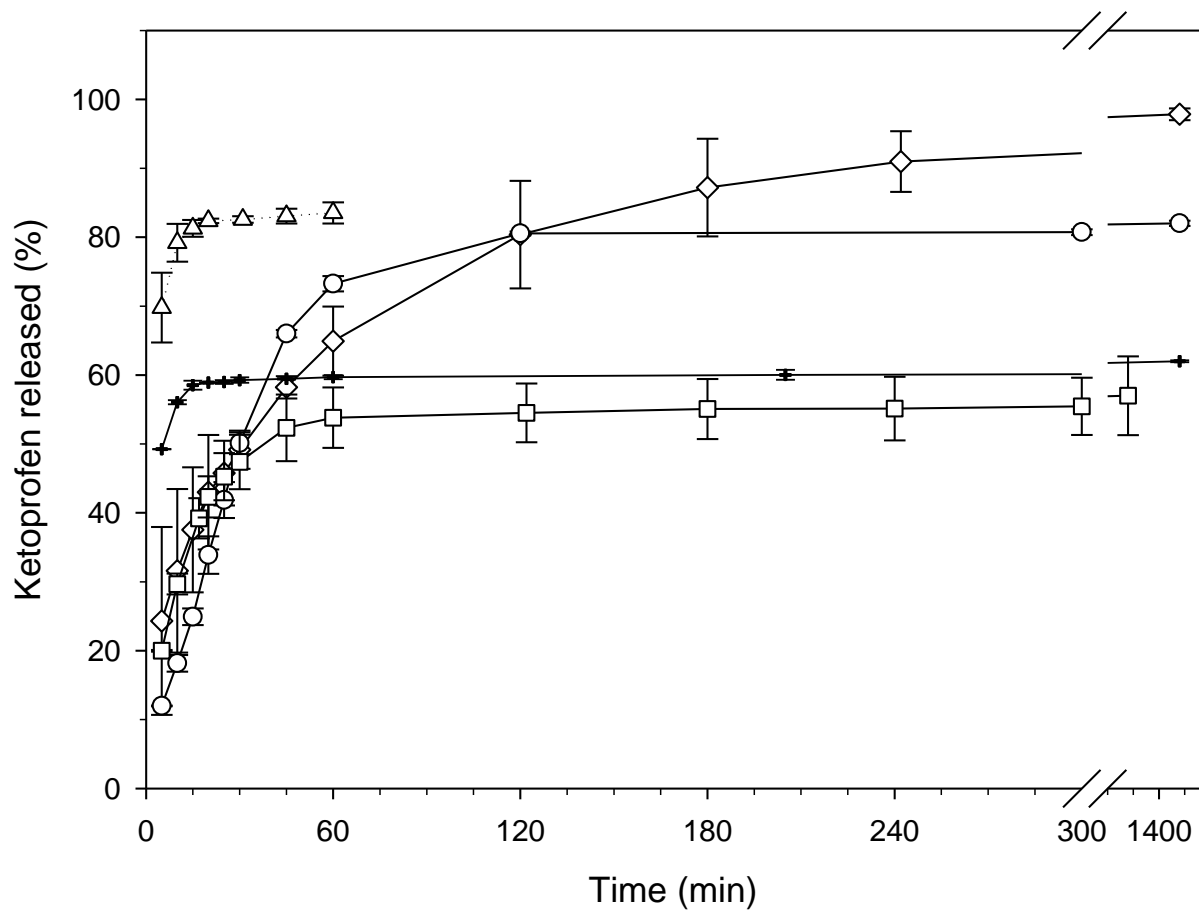
39

40

41

FIGURE 4

42
43
44
45



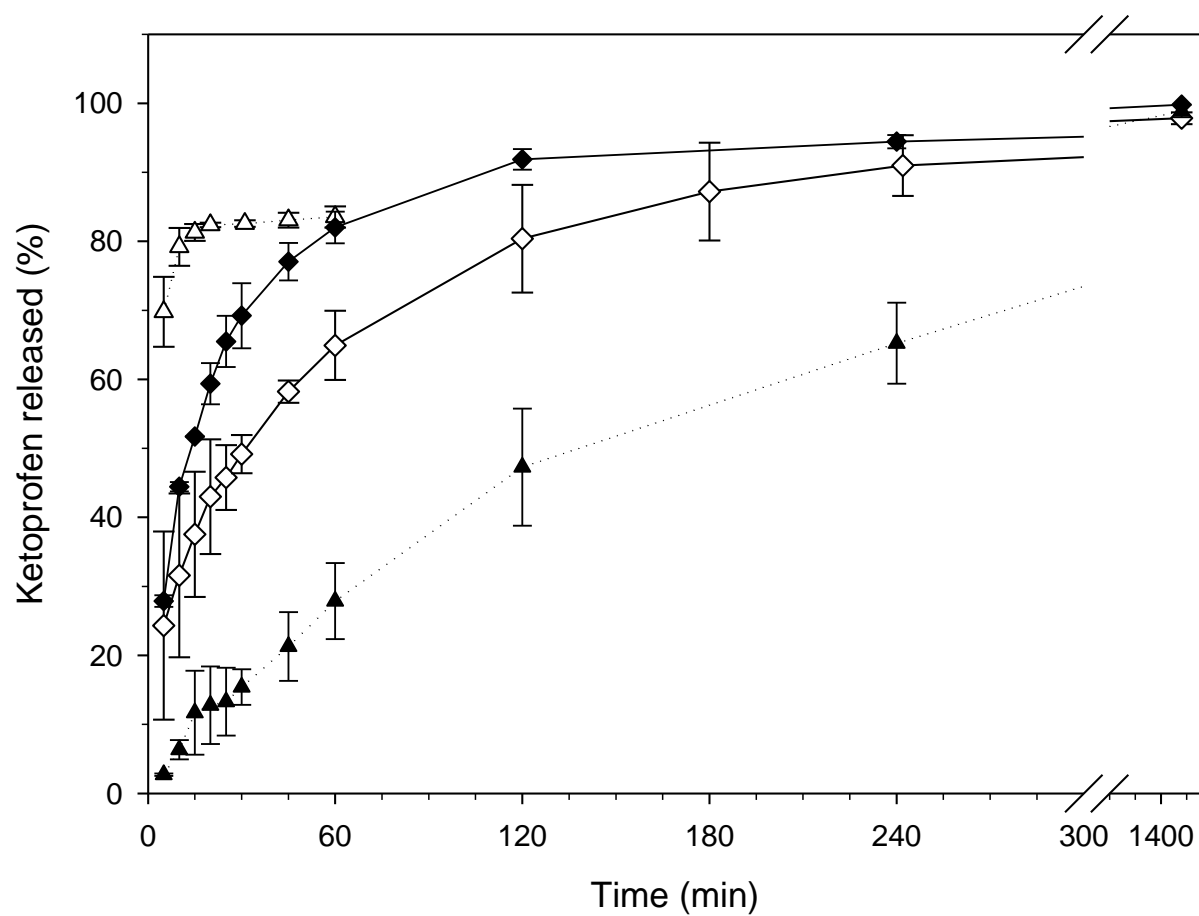
46
47
48
49
50
51

FIGURE 5

52

53

54



55

56

57

58

59

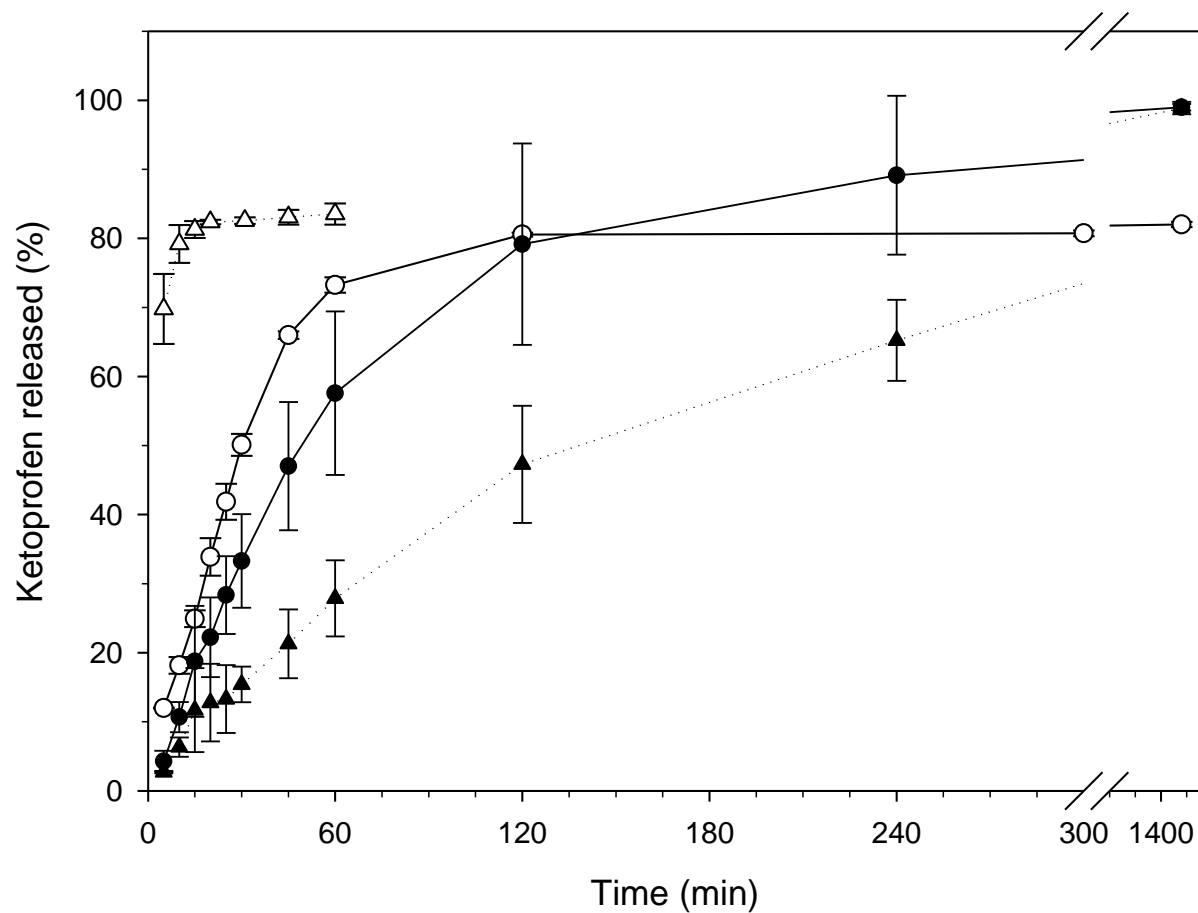
60

61

62

FIGURE 6

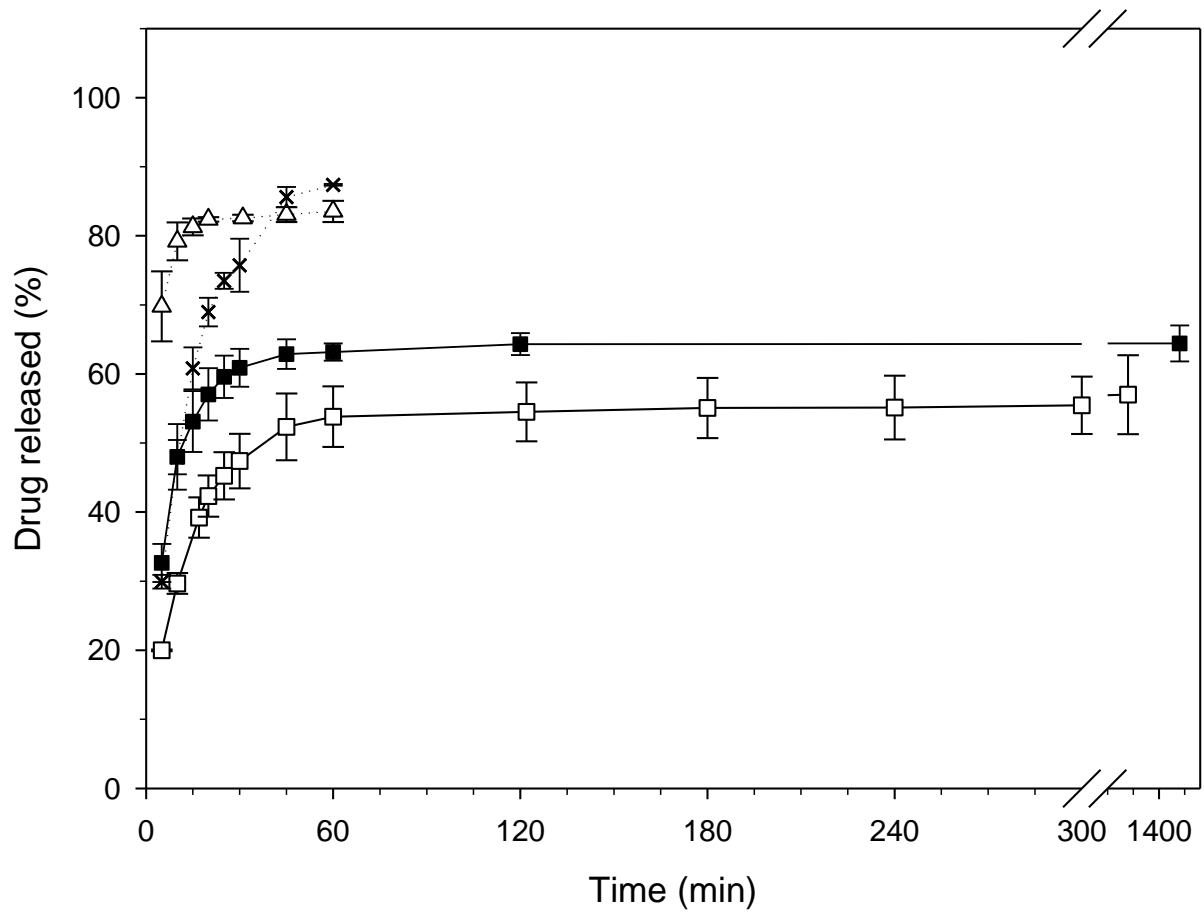
63
64
65
66



67
68
69
70
71
72
73

FIGURE 7

74
75
76



77
78
79
80
81
82
83

FIGURE 8

SUPPLEMENTARY DATA

A. Preparation of spherical aerogel microspheres [1]

A.1 Pectin aerogel [2]

Aerogel microspheres were obtained by stirring (500 rpm) an aqueous phase containing 6% (w/w) of pectin with the corresponding amount of canola oil to get a 3:1 (v/v) oil:pectin solution emulsion. Ethanol (50 wt% with respect to water content) was then added and the mixture was heated to 313 K for 30 min under agitation (500 rpm). Then, the system was cooled down to room temperature and continuously stirred at 2000 rpm. The dispersion was centrifuged to separate the pectin microparticles from the oil phase, immersed in 99.8% (v/v) EtOH and stored at room temperature during 24 h for aging. After a second solvent exchange to ethanol, the pectin gel was supercritically dried at 318 K, 11.0-12.0 MPa and CO₂ flow of 2-4 NL·min⁻¹ during 4 h.

A.2 Alginate aerogel [3]

A 2 % (w/w) alginate aqueous solution-in-paraffin oil emulsion (2:1 (v/v) oil:alginate solution) was prepared upon stirring (1000 rpm) at room temperature for 15 min. Prior to the emulsification, CaCO₃ was added to the alginate solution (Ca²⁺/alginate=7.3 wt%) and Span 80 surfactant (surfactant:oil volume ratio=1:99) was added to the oil phase. Gelation of the dispersed phase took place through the internal setting method by the addition of glacial acetic acid (acid-to-Ca²⁺ molar ratio=3.5). Gel microspheres were isolated through centrifugation and exposed to ethanol in a sequential solvent exchange (ethanol:water volume ratio 10:90, 30:70, 50:50, 70:30, 90:10, 99.99:0.01). Finally, aerogel microspheres were obtained by scCO₂-assisted drying (318 K, 11.0-12.0 MPa, 2-4 NLCO₂·min⁻¹, 4 h).

A.3 Starch aerogel [4]

A 2:1 volume phase ratio of a 15 % (w/w) corn starch dispersion in the corresponding amount of vegetable oil was prepared. The emulsion was heated in an autoclave to 393 K upon stirring (500 rpm) for 20 min. The emulsion was cooled down to room temperature while stirring at 2000 rpm. Then, the particles were centrifuged to remove the oil and water phase, soaked in ethanol and then stored at 277 K for retrogradation during 48h. After a second solvent exchange to ethanol, the starch gel was supercritically dried at 318 K, 11.0-12.0 MPa and CO₂ flow of 2-4 NL·min⁻¹ during 4 h.

A.4 Silica aerogel [5,6]

The sol (dispersed phase) was prepared in two steps: 1) Preparation of a TMOS:MeOH:water:HCl mixture with a molar ratio of 1:2.4:1.3:10⁻⁵ and dilution in ethanol; 2) Addition of water and ammonia solution to obtain a TMOS:MeOH:water:HCl:NH₄OH mixture with a molar ratio of 1:2.4:4:10⁻⁵:10⁻². The dispersed phase was mixed with the continuous phase (canola oil saturated with ethanol) to form the emulsion (sol:oil phase volume ratio=1:1) and stirred at 1300 rpm and room temperature for 20-30 min. After 24 h aging, the silica gel was filtered to remove the oil phase and then supercritically dried at 318 K, 11.0-12.0 MPa and CO₂ flow of 2-4 NL·min⁻¹ during 4h.

[1] García-González, C. A., Alnaief, M., & Smirnova, I. (2011). Polysaccharide-based aerogels - Promising biodegradable carriers for drug delivery systems. *Carbohydrate Polymers*, 86(4), 1425-1438.

[2] García-González, C. A., Carenza, E., Zeng, M., Smirnova, I., & Roig, A. (2012). Design of biocompatible magnetic pectin aerogel monoliths and microspheres. *RSC Advances*, 2(26), 9816-9823.

[3] Alnaief, M., Alzaitoun, M. A., García-González, C. A., & Smirnova, I. (2011). Preparation of biodegradable nanoporous microspherical aerogel based on alginate. *Carbohydrate Polymers*, 84(3), 1011-1018.

[4] García-González, C. A., Uy, J. J., Alnaief, M., & Smirnova, I. (2012). Preparation of tailor-made starch-based aerogel microspheres by the emulsion-gelation method. *Carbohydrate Polymers*, 88(4), 1378-1386.

[5] Alnaief, M., & Smirnova, I. (2011). In situ production of spherical aerogel microparticles. *The Journal of Supercritical Fluids*, 55(3), 1118-1123.

[6] García-González, C. A., Camino-Rey, M. C., Alnaief, M., Zetzl, C., & Smirnova, I. (2012). Supercritical drying of aerogels using CO₂: Effect of extraction time on the end material textural properties. *The Journal of Supercritical Fluids*, 66, 297-306.